Electron Beam Stimulated Molecular Motions

Ke Ran,[†,‡] Jian-Min Zuo,[‡,*] Qing Chen,[†,*] and Zujin Shi[§]

[†]Key Laboratory for Physics and Chemistry of Nanodevices and Department of Electronics, Peking University, Beijing 100871, People's Republic of China, [‡]Department of Material Science and Engineering and Materials Research Laboratory, University of Illinois at Urbana—Champaign, Urbana, Illinois 61801, United States, and [§]College of Chemistry and Molecular Engineering, Peking University, Beijing 100871, People's Republic of China

ABSTRACT Electron microscopy with advances in aberration correction has the power to resolve atoms in single molecules. However, its application is limited by electron irradiation induced molecular motions. A better understanding of damage mechanisms is required to achieve the full potential of electron imaging. Here, we report a direct observation of molecular motions stimulated by an electron beam, which allows us to study the breakdown and formation of molecular bonds using C_{60}'s encapsulated inside single-walled carbon nanotubes as a model system. An activation energy of 100 s meV is estimated for the observed molecular motions based on van der Waals interactions. We demonstrate that the molecular confinement can significantly increase the electron energy threshold for breaking the vdW bonds.

KEYWORDS: C_{60} · carbon nanotube · motion · van der Waals interaction · elastic scattering

Atomic resolution imaging of single molecules presents an ultimate challenge in the study of molecular nanostructures, including biological macromolecules.[1−3] Transmission electron microscopy is an excellent tool for direct observation of nanostructures at angstrom resolution. However, electron molecular imaging is limited by the undesirable effects of electron beam irradiation.[4−7] During the interaction between incident electrons and sample, part of the incident electrons' energy can be transferred to the sample by exciting bonded electrons or by electron scattering.[8,9] Electron excitation leads to irradiation damage by ionization of individual atoms, generation of phonons, or breaking and forming of chemical bonds in the sample.[10] During electron scattering, energy transferred is dependent on the incident electron energy and the scattering angle.[8] Once the energy transferred exceeds the displacement energy of the atom, knock-on damage takes place. A threshold energy for the knock-on damage was reported to be 100−140 keV for sp^2-bonded carbon atoms.[8,11] Reducing the electron beam knock-on damage has been the driving force toward the development of lower acceleration voltage, aberration-corrected TEMs.[12,13]

Molecules have a range of chemical bonds, and the intermolecular van der Waals (vdW) bonds are the weakest one. Here, we use C_{60}'s encapsulated inside carbon nanotubes (CNTs) (peapods) to study electron beam irradiation effects on vdW bonding. A previous study has shown that the CNT provides an ideal host to investigate the behavior of various molecules in a confined one-dimensional space.[14] For example, several kinds of chemical reactions[15,16] and molecular motions[17−20] have been reported in peapods. This work focuses on the range of molecular motions of the vdW-bonded C_{60} molecules that can be stimulated by electron beam irradiation. We report the observation of a single fullerene's jump in a defective zigzag C_{60} molecular chain, back and forth translation of a cluster of C_{60}'s in a partially filled CNT, pickup of C_{60} molecules, and rotation of a zigzag chain of C_{60}'s accompanied by deformation of the host CNT. Using a simple model of vdW potential among C_{60} molecules and the host CNT, we estimated the activation energies for some of the molecular motions, ranging from ~0.3 to 0.7 eV. These energies allow us to calculate the probability of electron scattering required to activate the molecular motions and to estimate the electron energy and electron beam current density allowed for electron molecular imaging.

All TEM observations were conducted under 80 kV electron beam irradiation. The electron acceleration voltage was selected to avoid the knock-on damage of the C−C sp^2 bonds.[21,22] Details of the experiment including the sample preparation are described in the Experimental Method section. Modeling of the interaction among C_{60}'s and the host CNT was carried out using the Lennard-Jones (LJ)-type vdW potential,[23] which has shown excellent agreement with a number of experimental studies of vdW bonding in carbon materials.[24,25]

* Address correspondence to jianzuo@uiuc.edu (J.M.Z.); qingchen@pku.edu.cn (Q.C.).

Received for review February 20, 2011 and accepted March 23, 2011.

Published online March 23, 2011
10.1021/nn2006909

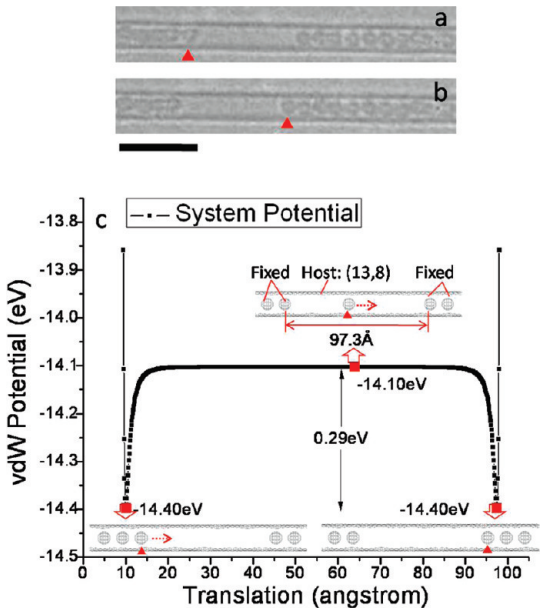

Figure 1. (a, b) Recorded TEM images showing the beginning and ending of a single C_{60}'s jump in an isolated peapod recorded with an exposure time of 0.5s. The two images are 0.5 s apart. The scale bar is 5 nm. (c) Calculated van der Waals potential energy for the jumping of a single C_{60} using the models illustrated in the insets.

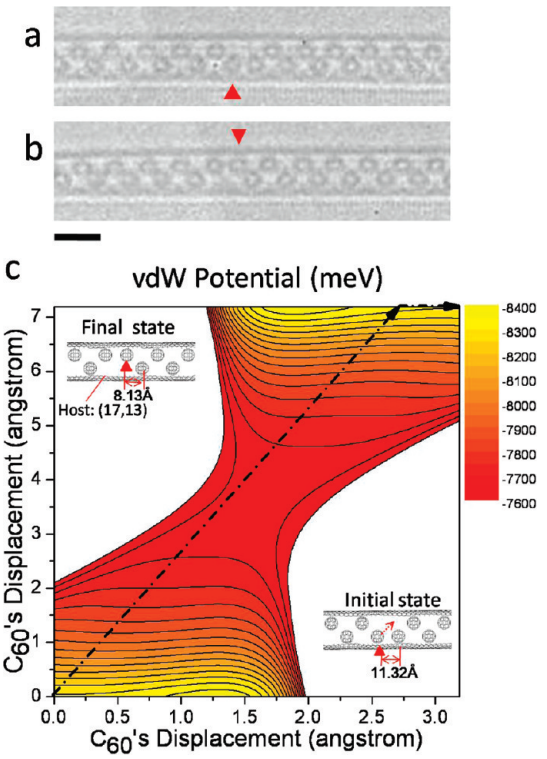

Figure 2. (a, b) Recorded TEM images before and after the jump of a single C_{60} at a defect site in a zigzag C_{60} chain. The exposure time is 1 s. The images are 5 s apart. The scale bar is 2 nm. (c) Calculated van der Waal potential energy of the peapod (in meV) as a function of the hopping C_{60}'s displacement. The *x*- and *y*-coordinates correspond to the displacement parallel and perpendicular to the tube axis, respectively. Insets are the structural models at the initial and final states used for the calculation.

RESULTS AND DISCUSSION

Translation of Single C_{60}. Single C_{60} was found to translate along the tube axis in a partially filled CNT under electron beam irradiation, as shown in Figure 1a,b. The images were captured at 0.5 s apart, which was not fast enough to record the intermediate stages of the molecular jump.[16] Figure 1c plots vdW potential of the peapod system calculated as a function of the moving C_{60}'s positions. The peapod model used for the vdW potential calculation was constructed using about the same tube diameter as the CNT observed in experiment. The calculations show that the chiral vector of the CNT has very little effect on the potential of a moving C_{60} inside the CNT.[26,27] Local minima and a local maximum are highlighted in the potential curve with their corresponding structural models. According to Figure 1c, an activation energy around 0.3 eV[19,20,28] is required to break the vdW bonding of a C_{60} at the end of a C_{60} molecular chain. After detachment, the C_{60} can move almost freely inside the CNT.

Single Molecular Jump. Figure 2a,b show a marked C_{60} (by the red triangle) at a defect site of a zigzag molecular chain of C_{60}'s. During the interval between the two images, the marked C_{60} jumped from one side to the other side of the chain without introducing obvious effects to the neighboring C_{60} molecules. Measurement of the inter C_{60}'s spacing indicates that the C_{60}'s jump is accompanied by a small translation parallel to the tube axis. Figure 2c plots the contour map of the calculated vdW potential as a function of the C_{60}'s displacement. *x*- and *y*-coordinates correspond to the C_{60}'s displacement parallel and perpendicular to the tube axis, respectively. The lower left and upper right corners represent the observed initial and final positions of the hopping C_{60}. In Figure 2c, the calculated energy minima for the initial and final states are deviated from these two corners, which could be due to the thermal energy or excitation of C_{60} by the electron beam irradiation. One possible path of the C_{60}'s hopping is marked by the black dashed arrow. Along it, a minimum ~0.7 eV in energy is required to drive the motion, which is much higher than the activation energy for the translation of a single C_{60} as observed in Figure 1.

Translation and Rotation of a Chain of C_{60}'s. A chain of C_{60}'s performed both translation and rotation inside a partially filled CNT, as shown in Figure 3a–j. Initially, in Figure 3a, a molecular chain of five C_{60}'s (in the red brackets) was observed at a middle position of the hollow space. Then, the molecular chain moved to the left side, accompanied by an obvious change in its configuration, which appears to be the result of molecular chain's rotation around the tube axis, as shown in Figure 3b. Meanwhile, another C_{60} (marked by the red triangle in Figure 3b) was attached to the chain. The newly formed chain of six C_{60}'s continued to change its configuration under the electron beam but without obvious translation during the recording period in Figure 3c,d. In Figure 3e, the molecular chain then moved and got trapped in the middle for about 1 s. After arriving

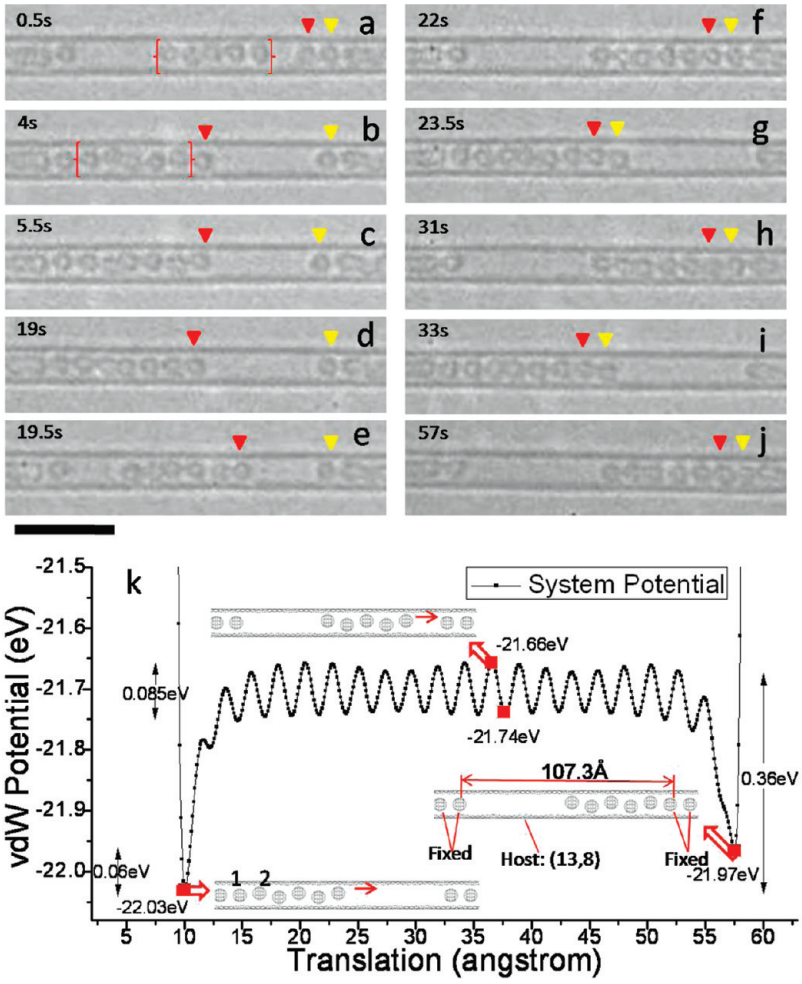

Figure 3. (a–j) Time series of TEM images captured from a video showing back and forth translations of a small chain of C_{60}'s. The recording lasted for 1 min, and 120 frames in total were recorded with an exposure time of 0.5 s. The scale bar is 5 nm. (k) Calculated van der Waals potential energy for the translation of a chain of five C_{60}'s inside a CNT. The structural models used for the calculation is shown in insets for three different positions.

at the right side and picking up one more C_{60} (marked by the yellow triangle) in Figure 3f, a chain of seven C_{60}'s formed and translated back and forth several times, as captured in Figure 3g–j. Figure 3k plots the calculated vdW potential based on the position of a five-C_{60} molecular chain. To mimic the experimental observation, the C_{60} chain has a small zigzag arrangement and is allowed to translate along the tube axis. The *x*-coordinate represents separation between the two C_{60} molecules marked as 1 and 2 in the peapod model (lower left in Figure 3k). The estimated activation energy, based on the constructed model, is ~0.36 eV (the activation energy is slightly dependent on the C_{60} orientations, which can introduce a difference of about 0.03 eV). A number of local minima and maxima show up in the middle part of the potential curve with energy barriers of ~0.085 eV, which have to be overcome to keep the C_{60} chain moving continuously inside the single-walled CNT.

Rotation of a Chain of C_{60}'s in an Overloaded CNT. Figure 4a–f show an overloaded peapod with a high line density of C_{60}'s. In Figure 4a, the C_{60} chain appears in a compact and almost linear configuration. Under electron beam irradiation, a part of the C_{60} molecular chain rotated about the tube axis, with a clear increase in the local projected CNT width, in Figure 4b. The molecular chain was seen in a zigzag arrangement. Separation between neighboring C_{60}'s in the zigzag direction is comparable to or larger than the CNT's original diameter, which contributes to the deformation seen in the CNT. This observation is followed by another rotation accompanied by a decrease of the CNT projected width in Figure 4c. The swell-and-shrink sequence repeated for a couple of times more, as shown in Figure 4d–f. In Figure 4g, the local width of the CNT around positions A and B, as marked in Figure 4a, was measured at different times. The changes in the observed CNT width can be explained by the elliptical deformation of the host CNT's cross section. As the zigzag C_{60} chain rotates, the deformation follows, which gives rise to alternate contraction and expansion in projection. The maximum expansion up to 29% was observed in Figure 4d at position A, corresponding to a diameter increase of 0.44 nm.

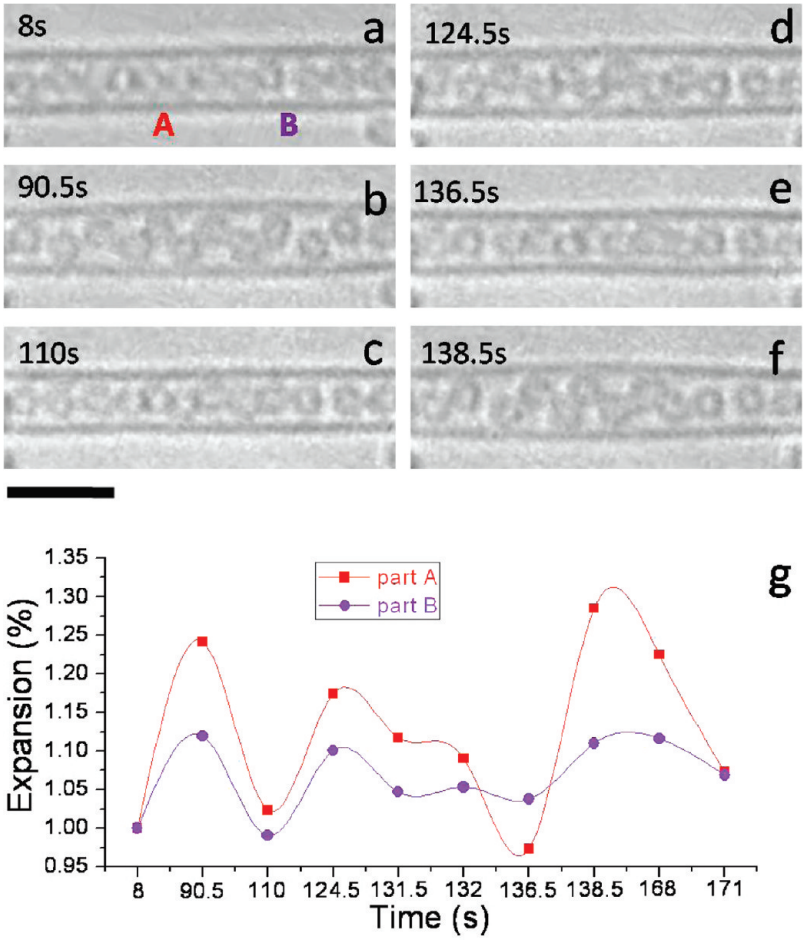

Figure 4. (a–f) Time series of TEM images captured from a video showing rotation of a zigzag C_{60} chain leading to expansion and contraction of the host CNT. The scale bar is 5 nm. (g) Measurement of the projected width of the host CNT at positions A and B as marked in (a) at different recording times.

Our work shows that different molecular motions of C_{60}'s require different activation energy ranging from ~0.3 to ~0.7 eV based on the vdW interaction. Somada *et al.*[19] and Ueno *et al.*[29] suggested that the activation energy may come from thermal energy. For this to occur, the temperature has to be as high as 4000 K to activate the single C_{60}'s translation in Figure 1. However, the peapod was reported to be an excellent thermal conductor,[30] and an estimation of the sample heating by electron beam irradiation predicted a rise of only less than 1 K above the experimental temperature (~300 K).[31] Thermal gradient driven motion was proposed by Barreiro *et al.*[20] and Zambrano *et al.*[28] In their work, a steady thermal gradient was imposed on the sample to drive the molecular motion through momentum transferred from the phonon excitation.[20] However, in our experiment, considering the lack of temperature rise and relatively uniform illumination during TEM observation,[32] it is unlikely to generate the similar steady thermal gradient in the sample. Moreover, molecular motions driven by the thermal gradient are expected to be directed toward a specific direction, from hot spots to cold regions, which is not consistent with the back and forth translations nor the rotation of the C_{60} molecules.

Thus, the activation energy for those observed molecular motions can only come from electron scattering with a significant amount of momentum transfer. In TEM, incident electrons are scattered by atoms in the sample either elastically or inelastically through the Coulomb interaction.[8] Large angle elastic scattering gives rise to large momentum transfer. Because the C_{60}'s are confined in a one-dimensional space, only momentum transferred along a specific direction can drive the observed translation. The average momentum transferred from an incident electron to a carbon atom of a C_{60} along the tube axis is given by

$$\langle P \rangle = 2 \times \frac{1}{2\pi} \int_0^{\pi/2} m_e \sin\theta \times v_0 \cos\varphi \, d\varphi = \frac{m_e \sin\theta \times v_0}{\pi} \quad (1)$$

corresponding to an amount of energy

$$\langle E_{||} \rangle = \frac{{m_e}^2 \sin^2\theta \times v_0^2}{2 m_a \pi^2} \quad (2)$$

where m_e, θ, and v_0 are the mass, scattering angle, and initial velocity of the incident electron, m_a is the mass of a

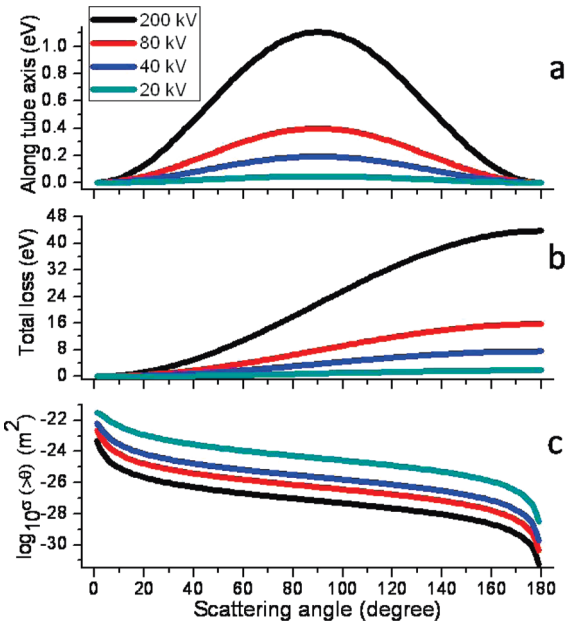

Figure 5. Energy loss of each incident electron based on the momentum transfer along the tube axis (a) and in an arbitrary direction (total energy loss) (b). (c) Logarithm of the scattering cross section of an incident electron scattered beyond a given scattering angle (*x*-axis) for different electron acceleration voltages.

carbon atom, and φ is the angle between the tube axis and the plane defined by the momenta of the incident electrons and the carbon atom. Figure 5a plots $\langle E_{\parallel} \rangle$ as a function of θ for different incident electron energies. The maximum $\langle E_{\parallel} \rangle$ is obtained by scattering the incident electron into 90°. In comparison, the total energy transferred, $\langle E \rangle$, is

$$\langle E \rangle = \frac{2m_e{}^2 \sin^2(\theta/2) \cdot v_0{}^2}{m_a} \qquad (3)$$

which has a maximum at 180° (Figure 5b).[8]

According to the above equations, for the translation of a C_{60} molecular cluster as observed in Figure 3a–j, the scattering angle θ should be greater than 72° in order to transfer the required activation energy (~0.36 eV). The probability of a scattering event is described by its cross section, $\sigma(\theta)$, which can be obtained by integrating the differential cross section,[9]

$$\frac{d\sigma(\theta)}{d\Omega} = \frac{\lambda_R{}^4 Z^2}{64\pi^4 (a_0)^2 (\sin^2(\theta/2) + (\theta_0/2)^2)^2} \qquad (4)$$

from θ to π. Figure 5c plots the logarithm of $\sigma(\theta)$ as a function of θ under different electron energies. The probability decreases as the scattering angle and the incident electron energy increase. For $\theta \approx 72°$, the scattering cross section ($\sigma(\theta) \geq 72°$) is ~0.03% of the total scattering cross section (2.1×10^{-4} nm^2) at 80 kV. With an electron dose of 3×10^5 e/s·nm^2, the chance for a C_{60} to suffer this kind of scattering can be estimated to be around 1 time per second. During the experiment, the observed frequency of the back and forth translation is 6/min, which is far below the estimated value. Although due to the limited temporal resolution of the microscope, only slow molecular motions are observed.

The maximal energy transfer parallel to the tube axis (eq 2, with $\theta = 90°$) is one of $4\pi^2$ of the maximal total energy that can be transferred (eq 3, with $\theta = 180°$). Taking the back and forth translation for example, parallel energy transfer provides a threshold for the incident electron energy at 72 kV for 0.36 eV loss. In comparison, the total energy transfer has a threshold of 1.83 kV for the same energy loss. Thus, for electron molecular imaging, molecular confinement will help the atomic resolution imaging of molecules at medium electron high voltages. Under electron beam irradiation, intermolecular bonding or charge transfer may take place as well to induce the so-called ionization damage. Electron high voltages help reduce the ionization damage.

In summary, we report single C_{60} jump and translation as well as translation and rotation of a C_{60} molecular chain. Host CNT expansion up to 29% induced by rotation of a zigzag C_{60} chain has also been observed. On the basis of van der Waals potential simulation of simple models, we show that these observed molecular motions require ~0.3 to ~0.7 eV. The lowest activation energy is associated with a single C_{60} detachment at the end of a C_{60} molecular chain, while the largest activation energy is associated with the molecular jump at a defect site. This result suggests molecular vacancies can lead to lower activation energy and one-dimensional confinement can significantly increase the electron beam energy threshold for breaking the bonds. For imaging confined C_{60}'s, the optimum electron energy predicted is ~60 kV.

EXPERIMENTAL METHOD

Single-walled carbon nanotubes used in our experiments were synthesized by the arc discharge method. A mixture of SWCNT and C_{60} powder was put into a glass tube connected to a vacuum pump. During pumping, the glass tube was heated to 573 K for 2 h to get rid of the gas molecules adsorbed on the SWCNT, and then the glass tube was sealed at 10^{-4} Pa and gradually heated and kept at 723 K for 48 h. The highly filled peapods were obtained and then dispersed in *N*,*N*-dimethyl formamide for ultrasonic treatment. A lacey carbon film on a copper grid obtained from Ted Pella Inc. was used to support the peapods for TEM observation.

To avoid knock-on damage, all TEM observations in this work were performed using a JEOL 2200FS TEM with a field emission gun at a voltage of 80 kV and an electron beam dose of 3×10^5 e/s·nm^2 at room temperature.

Acknowledgment. This work was supported by NSF of China (60728102 and 60925003) and DOE (DEFG02-01ER45923). K.R. acknowledges fellowship support from CSC (China). Microscopy was carried out at the Frederick Seitz Materials Research Laboratory Central Facilities, University of Illinois.

Supporting Information Available: Movies showing back and forth translations and rotation of C_{60} chains. This material is available free of charge *via* the Internet at http://pubs.acs.org.

REFERENCES AND NOTES

1. Koshino, M.; Niimi, Y.; Nakamura, E.; Kataura, H.; Okazaki, T.; Suenaga, K.; Iijima, S. Analysis of the Reactivity and Selectivity of Fullerene Dimerization Reactions at the Atomic Level. *Nat. Chem.* **2010,** *2*, 117–124.
2. Hashimoto, A.; Suenaga, K.; Gloter, A.; Urita, K.; Iijima, S. Direct Evidence for Atomic Defects in Graphene Layers. *Nature* **2004,** *430*, 870–873.
3. Meyer, J. C.; Kisielowski, C.; Erni, R.; Rossell, M. D.; Crommie, M. F.; Zettl, A. Direct Imaging of Lattice Atoms and Topological Defects in Graphene Membranes. *Nano Lett.* **2008,** *8*, 3582–3586.
4. Urita, K.; Suenaga, K.; Sugai, T.; Shinohara, H.; Iijima, S. *In situ* Observation of Thermal Relaxation of Interstitial-Vacancy Pair Defects in a Graphite Gap. *Phys. Rev. Lett.* **2005,** *94*, 155502–4.
5. Gloter, A.; Suenaga, K.; Kataura, H.; Fujii, R.; Kodama, T.; Nishikawa, H.; Ikemoto, I.; Kikuchi, K.; Suzuki, S.; Achiba, Y.; *et al.* Structural Evolutions of Carbon Nano-Peapods under Electron Microscopic Observation. *Chem. Phys. Lett.* **2004,** *390*, 462–466.
6. Hernandez, E.; Meunier, V.; Smith, B. W.; Rurali, R.; Terrones, H.; Nardelli, M. B.; Terrones, M.; Luzzi, D. E.; Charlier, J. C. Fullerene Coalescence in Nanopeapods: A Path to Novel Tubular Carbon. *Nano Lett.* **2003,** *3*, 1037–1042.
7. Krasheninnikov, A. V.; Nordlund, K. Ion and Electron Irradiation-Induced Effects in Nanostructured Materials. *J. Appl. Phys.* **2010,** *107*, 071301–70.
8. Egerton, R. F.; Li, P.; Malac, M. Radiation Damage in the TEM and SEM. *Micron* **2004,** *35*, 399–409.
9. Williams, D. B.; Carter, C. B. *Transmission Electron Microscopy*; Springer: New York, 2009; Vol. 1.
10. Banhart, F. Irradiation Effects in Carbon Nanostructures. *Rep. Prog. Phys.* **1999,** *62*, 1181–1221.
11. Krasheninnikov, A. V.; Banhart, F. Engineering of Nanostructured Carbon Materials with Electron or Ion Beams. *Nat. Mater.* **2007,** *6*, 723–733.
12. Sasaki, T.; Sawada, H.; Hosokawa, F.; Kohno, Y.; Tomita, T.; Kaneyama, T.; Kondo, Y.; Kimoto, K.; Sato, Y.; Suenaga, K. Performance of Low-Voltage STEM/TEM with Delta Corrector and Cold Field Emission Gun. *J. Electron Microsc.* **2010,** *59*, S7–S13.
13. Krivanek, O. L.; Chisholm, M. F.; Nicolosi, V.; Pennycook, T. J.; Corbin, G. J.; Dellby, N.; Murfitt, M. F.; Own, C. S.; Szilagyi, Z. S.; Oxley, M. P.; *et al.* Atom-by-Atom Structural and Chemical Analysis by Annular Dark-field Electron Microscopy. *Nature* **2010,** *464*, 571–574.
14. Smith, B. W.; Monthioux, M.; Luzzi, D. E. Encapsulated C-60 in Carbon Nanotubes. *Nature* **1998,** *396*, 323–324.
15. Chuvilin, A.; Khlobystov, A. N.; Obergfell, D.; Haluska, M.; Yang, S. H.; Roth, S.; Kaiser, U. Observations of Chemical Reactions at the Atomic Scale: Dynamics of Metal-Mediated Fullerene Coalescence and Nanotube Rupture. *Angew. Chem., Int. Ed.* **2010,** *49*, 193–196.
16. Warner, J. H.; Ito, Y.; Rummeli, M. H.; Buchner, B.; Shinohara, H.; Briggs, G. A. D. Capturing the Motion of Molecular Nanomaterials Encapsulated within Carbon Nanotubes with Ultrahigh Temporal Resolution. *ACS Nano* **2009,** *3*, 3037–3044.
17. Warner, J. H.; Ito, Y.; Rummeli, M. H.; Gemming, T.; Buchner, B.; Shinohara, H.; Briggs, G. A. D. One-Dimensional Confined Motion of Single Metal Atoms inside Double-Walled Carbon Nanotubes. *Phys. Rev. Lett.* **2009,** *102*, 195504–4.
18. Warner, J. H.; Ito, Y.; Zaka, M.; Ge, L.; Akachi, T.; Okimoto, H.; Porfyrakis, K.; Watt, A. A. R.; Shinohara, H.; Briggs, G. A. D. Rotating Fullerene Chains in Carbon Nanopeapods. *Nano Lett* **2008,** *8*, 2328–2335.
19. Somada, H.; Hirahara, K.; Akita, S.; Nakayama, Y. A Molecular Linear Motor Consisting of Carbon Nanotubes. *Nano Lett.* **2009,** *9*, 62–65.
20. Barreiro, A.; Rurali, R.; Hernandez, E. R.; Moser, J.; Pichler, T.; Forro, L.; Bachtold, A. Subnanometer Motion of Cargoes Driven by Thermal Gradients along Carbon Nanotubes. *Science* **2008,** *320*, 775–778.
21. Hobbs, L. W. Electron-Beam Sensitivity in Inorganic Specimens. *Ultramicroscopy* **1987,** *23*, 339–344.
22. Warner, J. H.; Schaffel, F.; Zhong, G. F.; Rummeli, M. H.; Buchner, B.; Robertson, J.; Briggs, G. A. D. Investigating the Diameter-Dependent Stability of Single-Walled Carbon Nanotubes. *ACS Nano* **2009,** *3*, 1557–1563.
23. Hodak, M.; Girifalco, L. A. Fullerenes inside Carbon Nanotubes and Multi-Walled Carbon Nanotubes: Optimum and Maximum Sizes. *Chem. Phys. Lett.* **2001,** *350*, 405–411.
24. Jiang, Y. Y.; Zhou, W.; Kim, T.; Huang, Y.; Zuo, J. M. Measurement of Radial Deformation of Single-Wall Carbon Nanotubes Induced by Intertube van der Waals Forces. *Phys. Rev. B* **2008,** *77*, 153405–4.
25. Chen, B.; Gao, M.; Zuo, J. M.; Qu, S.; Liu, B.; Huang, Y. Binding Energy of Parallel Carbon Nanotubes. *Appl. Phys. Lett.* **2003,** *83*, 3570–3571.
26. Hodak, M.; Girifalco, L. A. Ordered Phases of Fullerene Molecules Formed inside Carbon Nanotubes. *Phys. Rev. B* **2003,** *67*, 075419–4.
27. Liu, P.; Zhang, Y. W.; Gao, H. J.; Lu, C. Energetics and Stability of C-60 Molecules Encapsulated in Carbon Nanotubes. *Carbon* **2008,** *46*, 649–655.
28. Zambrano, H. A.; Walther, J. H.; Koumoutsakos, P.; Sbalzarini, I. F. Thermophoretic Motion of Water Nanodroplets Confined inside Carbon Nanotubes. *Nano Lett.* **2009,** *9*, 66–71.
29. Ueno, Y.; Somada, H.; Hirahara, K.; Nakayama, Y.; Akita, S. Molecular Dynamics Simulations for Molecular Linear Motor Inside Nanotube. *Jpn. J. Appl. Phys.* **2009,** *48*, 06FG03–3.
30. Noya, E. G.; Srivastava, D.; Chernozatonskii, L. A.; Menon, M. Thermal Conductivity of Carbon Nanotube Peapods. *Phys. Rev. B* **2004,** *70*, 115416–5.
31. Banhart, F. Irradiation of Carbon Nanotubes with A Focused Electron Beam in the Electron Microscope. *J. Mater. Sci.* **2006,** *41*, 4505–4511.
32. Reimer, L. *Transmission Electron Microscopy: Physics of Image Formation and Microanalysis*; Springer-Verlag: Berlin, 1984.